Journal of Current Science and Technology, April-June 2026 Vol. 16 No. 2, Article 173
Copyright ©2018-2026, Rangsit University
ISSN 2630-0656 (Online)

Cite this article: Phoophuangpairoj, R., & Charnkeitkong, P. (2026). A hybrid deep learning and machine learning approach for predicting aqueous solution concentrations. *Journal of Current Science and Technology*, *16*(2), Article 173. https://doi.org/10.59796/jcst.V16N2.2026.173

Journal of Current Science and Technology

Journal homepage: https://jcst.rsu.ac.th

A Hybrid Deep Learning and Machine Learning Approach for Predicting Aqueous Solution Concentrations

Rong Phoophuangpairoj[1], and Panida Charnkeitkong[2,*]

[1]Department of Computer Engineering, College of Engineering, Rangsit University, Pathum Thani 12000, Thailand
[2]Department of Chemical Engineering, College of Engineering, Rangsit University, Pathum Thani 12000, Thailand

*Corresponding author; E-mail: panida.s@rsu.ac.th

Received 7 August 2025; Revised 23 September 2025; Accepted 3 November 2025; Published online 25 March 2026

Abstract

Assessing solution concentration is essential across multiple scientific disciplines; however, it is often complicated by limitations in instrument precision, sample impurities, and environmental variables. Low concentration levels frequently necessitate sophisticated methods such as spectroscopy or chromatography, which require specific apparatus and expertise. Conventional methods might be laborious and occasionally inadequate for accurate measurements. Consequently, researchers continually develop better, more efficient, and economically viable methodologies. Recent technological advancements, including deep learning and machine learning, facilitate the development of efficient, cost-effective systems for determining solution concentration levels, applicable to environmental monitoring and food safety tests. Therefore, this research developed a methodology for estimating solution concentrations through deep learning feature extraction and machine learning-based prediction. Images of the solution at varying concentrations were used to train models that apply deep learning for feature extraction. Linear regression (LR), artificial neural network (ANN), support vector regression (SVR), and random forest (RF) were then evaluated for using the extracted features to forecast the concentrations. Using features extracted from Visual Geometry Group 16-layer Convolutional Neural Network (VGG16) with LR, ANN, SVR, and RF yielded absolute prediction errors of 0.056229, 0.080000, 0.112172, and 0.026640, respectively, for concentration class prediction (classes 1–10). When the concentrations of classes 1 to 10 were evenly changed from 0 ppm to 4500 ppm, using VGG16 to extract features and RF to predict concentrations resulted in an average absolute error of 13.32 ppm, an RMSE of 0.072531 (normalized class scale) and 36.31 ppm (concentration scale), and an R^2 of 0.999361. The findings indicated that the proposed inexpensive method could efficiently classify the solution in different concentration classes and forecast their concentrations.

Keywords: *deep learning; machine learning; random forest predictor; solution concentration; VGG16*

1. Introduction

The assessment of solution concentration is a crucial component of chemical analysis and is essential in numerous scientific disciplines, including chemistry, biology, environmental research, and pharmaceuticals. Evaluating solution concentration is essential across multiple scientific fields, although this process may be hindered by instrument accuracy limitations, sample impurities, and environmental factors. Traditional methods can be intricate, expensive, and time-consuming for such measurements. To address these issues, ongoing research aims to improve current procedures and develop innovative methodologies. Recent advancements encompass the use of automation, miniaturized sensors, and artificial intelligence, which collectively enhance data precision, reduce human error, and optimize analytical operations. Solution concentration analysis is complex and requires a strong understanding of chemical principles of chemical principles, dedication to experimental design, and continual advancement in analytical

technologies. In the absence of such endeavors, the precision and reliability of chemical analysis would be constrained, hindering advancement in various scientific fields. A nano/micro-structured pesticide detection card has been developed to fulfill food safety requirements. This card provides superior storage stability and a low detection limit, facilitating operation and reducing resource consumption compared with traditional approaches (Feng et al., 2021). Such assessment is crucial in chemical analysis, particularly for environmental monitoring, pharmaceuticals, and industrial quality control. Heavy metals, in the form of metallic ions, are of considerable concern due to their dual nature serving essential biological functions at trace levels but posing significant toxicological risks when present at elevated concentrations (Zhong et al., 2024). Traditional analytical methods such as titration and gravimetric analysis often lack the sensitivity and precision necessary to detect low concentrations of these elements (Paredes et al., 2023). To overcome these constraints, advanced analytical techniques, such as spectrophotometry, high-performance liquid chromatography (HPLC), and atomic absorption spectroscopy (AAS), have been widely employed due to their high sensitivity and selectivity (Sun et al., 2024; Xhanari & Finšgar, 2023). However, these techniques frequently demand expensive instrumentation and specialist skills, which can limit their accessibility in routine field applications (Han et al., 2025; Sharma et al., 2025).

The determination of aqueous solution concentration is an essential aspect of chemical analysis and is pivotal in various scientific fields, including environmental chemistry, food safety, toxicology, and materials science. Analyzing copper (Cu^{2+}) content, for example, is crucial for environmental monitoring, biomedical diagnostics, and industrial quality control, as precise measurement ensures that concentrations remain within permissible safety limits (Han et al., 2023). Conventional techniques can be laborious and occasionally inadequate for accurate measurements. Consequently, researchers continually develop novel, more efficient, and economically viable methodologies. Technological advancements such as automation and artificial intelligence enhance precision and efficiency, making analysis more reliable. The analysis of solution concentration presents intricate obstacles that necessitate continuous innovation to ensure precise and efficient outcomes. To address these limitations, increasingly sophisticated instrumental techniques are widely employed, such as atomic absorption spectroscopy (AAS), inductively coupled plasma mass spectrometry (ICP-MS), and high-performance liquid chromatography (HPLC). These technologies offer exceptional accuracy and detection thresholds as low as the nanomolar or parts per billion. Nonetheless, their application is limited by substantial equipment expenses, the requirement for specialized knowledge, labor-intensive sample preparation, and access to laboratory facilities (Han et al., 2023; Li et al., 2022). The incorporation of artificial intelligence and machine learning into spectroscopy and chromatography is transforming data analysis. Modern algorithms are now capable of correcting instrumental drift, optimizing peak detection, and improving quantitative predictions, thereby reducing human error and increasing analytical throughput. The integration of affordable sensors, mobile imaging, and AI-based processing holds significant potential for advancing rapid medical diagnostics and environmental monitoring (Guo et al., 2025).

Advancements in analytical chemistry have begun to address these constraints. Methods such as UV–Vis spectrophotometry using chromogenic reagents (e.g., diethyldithiocarbamate (DDTC), cuprizone), cloud point extraction, and microextraction techniques have facilitated rapid and portable detection of copper. Moreover, smartphone-based colorimetric sensing has garnered interest owing to its cost-effectiveness, ease of use, and versatility for field applications. Users can accurately estimate copper content by recording photos of color responses and evaluating RGB (Red, Green, Blue) or HSV (Hue, Saturation, Value) color values using calibration models. Image-based colorimetric techniques using smartphones have emerged as a promising alternative, offering low-cost, portable, and user-friendly solutions. These approaches utilize chemical processes that generate color changes according to copper concentration, subsequently evaluated by RGB or HSV values derived from collected photos. Moreover, advancements including miniaturized sensors and artificial intelligence-assisted data analysis have improved the reliability and application of copper detection across many settings.

A rapid detection method for pesticide residues in fruits and vegetables employing machine learning color recognition was investigated. Ten concentrations of pesticide residues were identified using the blue indicators on rapid pesticide-residue test strips. The method using an exponential loss function achieved a model fitting R^2 of 0.935 (Dai et al., 2025). Researchers investigated the development of rapid pesticide-

residue detection cards using the enzyme inhibition approach. The study used image processing techniques to derive RGB features from the rapid detection card's data, using regression models. The results showed that the exponential regression model excelled in forecasting pesticide residue levels, as evidenced by the rapid detection card. The correlation coefficient was 0.900, and the root mean square error was 0.106 (Zhang et al., 2023).

Techniques for image processing, such as threshold extraction and RGB value analysis to derive multicolor features, were employed for the color recognition of test strips in rapid pesticide residue detection (Dai et al. 2025). Nonetheless, feature extraction through image processing approaches requires specific methodologies that do not have the capability to learn from data. Advances in AI-enabled technologies, such as machine learning and deep learning, help improve current procedures and facilitate the development of new ones. Deep learning algorithms have advantages over traditional image processing methods and can effectively learn from data and readily adapt to new datasets. For color-based classification using deep learning, researchers employed Convolutional Neural Network (CNN), MobileNet, Visual Geometry Group 16-layer Convolutional Neural Network (VGG16), and ResNet50 for image classification. MobileNet, ResNet50, and basic CNN classifiers correctly identified banana ripeness with accuracies of 98.43%, 94.19%, and 95.35%, respectively (Chen & Phoophuangpairoj, 2024). Mango ripeness classification yielded accuracies of 85.11% for MobileNet, 73.66% for ResNet50, and 90.08% for VGG16 classifiers. The VGG16 attained the best classification accuracy (Dong & Phoophuangpairoj, 2024). Typically, MobileNet, VGG16, and ResNet50 were supplemented with a flattened layer, several hidden layers, and an output layer. On multiple occasions, the softmax output values were utilized to determine the classification classes. The softmax function is a mathematical operation that transforms a vector of raw prediction scores from the neural network into values that represent class probabilities.

Artificial neural networks (ANN), support vector regression (SVR), linear regression (LR), and random forest (RF) are widely used methods for classification and prediction tasks. RF has been effectively used to classify normal and dangerous motorcycling behaviors using pose landmarks extracted with You Only Look Once (YOLO) (Si & Phoophuangpairoj, 2025). Support vector machine (SVM) and ANN were used to classify weightlifting phases based on posture landmarks and barbell features extracted with MediaPipe and YOLO (Qi & Phoophuangpairoj, 2024). RF is an ensemble machine learning technique that combines multiple decision trees to enhance prediction accuracy. During training, it creates multiple trees using random subsets of the dataset and features. In the prediction phase, RF aggregates the results of these trees through a voting mechanism, leveraging insights from multiple trees to ensure reliable outcomes. LR formulates a linear model with coefficients aimed at minimizing the residual sum of squares between the observed targets and the anticipated targets. SVR is a machine learning technique employed for regression tasks, a category of supervised learning that builds upon the principles of SVM. ANN is a particularly useful tool for problems involving both regression and classification. RF, SVR, ANN, and LR with various hyper-parameters were employed to predict solution concentrations. As a result, affordable methods for determining solution concentration should be developed and tested.

2. Objectives

The objective of this work is to develop and evaluate accurate, cost-effective, and portable methodologies for determining aqueous solution concentrations, particularly the concentration of copper ions (Cu^{2+}), by integrating deep learning feature extraction with machine learning-based prediction. This study aims to address the limitations of traditional detection methods by utilizing artificial intelligence and a smartphone camera to enhance precision, reduce resource consumption, and enable rapid, field-deployable chemical analysis for environmental, biomedical, agricultural, and industrial applications.

3. Materials and Methods

3.1 Data

Solutions of copper (II) nitrate trihydrate ($Cu(NO_3)_2 \cdot 3H_2O$) were prepared at different concentrations for data collection. The concentrations for classes 1–10 were prepared at uniform intervals of 500 ppm, ranging from 0 ppm (Class 1, distilled water) to 4500 ppm (Class 10). To prepare solutions of varying concentrations for the 10 classes, we weighed DAEJUNG™ Copper (II) Nitrate Trihydrate 99% (Extra Pure) and added water to achieve the specified concentration, as described in Table 1. Solutions for each concentration class were prepared,

and the procedure was repeated three times to obtain three sets of solutions. The solutions were poured into 100 mL beakers. For each concentration class and each preparation, twenty images were taken under the same illuminance of approximately 350 lx. A total of six hundred images were taken, with 60 images for each class. These images were divided into a training set, a validation set, and a test set. The training set consisted of 400 images. Each class comprised 40 images. The validation set consisted of 100 images, with ten images per class. The test set comprised 100 images that were not part of the training or validation sets. Figure 1 displays images of solutions with ten distinct concentrations. An iPhone 13 mini was used to capture images of the ten different solution concentrations.

3.2 Methods

MobileNet, ResNet50, and VGG16 were implemented using Python, TensorFlow, and Scikit-learn, and their efficacy in classifying copper(II) nitrate trihydrate ($Cu(NO_3)_2 \cdot 3H_2O$) solutions into ten concentration classes was assessed. IBM SPSS Statistics Version 22 (Passport Advantage Customer: Rangsit University) was used to compute the paired *t*-test for comparing the means of true and predicted concentration values. Figure 2 shows the method applied to obtain a hybrid deep learning and machine learning approach for predicting aqueous solution concentrations. It consisted of two parts: 1) select the best deep learning concentration classifier and 2) select the best machine learning concentration predictor. In the second part, we used ten outputs from the final softmax layer of VGG16, the most accurate classifier, to predict concentration levels due to its exceptional accuracy in categorizing solutions into discrete classes. The experiments evaluated the effectiveness of MobileNet, ResNet50, and VGG16 in classifying the solutions to determine which model was optimal for feature extraction. Then the predictive efficacy of VGG16 softmax features in conjunction with LR, ANN, SVR, and RF was examined to propose an efficient method for the prediction of aqueous solution concentrations when solution color intensity changes with concentration.

MobileNet, ResNet50, and VGG16 were augmented with three layers. The first and second layers consisted of 256 and 128 nodes, respectively, and employed the rectified linear unit (ReLU) activation function. In the final layer, a softmax activation function was employed. Ten nodes were included, and L2 regularization with a penalty coefficient of 0.005 was applied. The models were trained with a batch size of 20, 300 epochs, and a 0.0001 learning rate. For prediction, max_features=n_features and n_estimator=1000 were used in the RF. The ANN with an output node and a hidden layer with 16 nodes was employed and trained for 500 epochs. C=1.0 and epsilon=0.1 were the Scikit-learn default values used in the study of SVMs with linear, polynomial, and radial basis function kernels.

Table 1 Preparation of copper(II) nitrate trihydrate solutions at ten concentration levels

Classes	Methods for preparing the solutions
1	Use distilled water.
2	A 500 ppm concentration solution was obtained by weighing 0.0500 g and adding water to obtain 100 mL of solution.
3	A 1,000 ppm concentration solution was obtained by weighing 0.1000 g and adding water to obtain 100 mL of solution.
4	A 1,500 ppm concentration solution was obtained by weighing 0.1500 g and adding water to obtain 100 mL of solution.
5	A 2,000 ppm concentration solution was obtained by weighing 0.2000 g and adding water to obtain 100 mL of solution.
6	A 2,500 ppm concentration solution was obtained by weighing 0.2500 g and adding water to obtain 100 mL of solution.
7	A 3,000 ppm concentration solution was obtained by weighing 0.3000 g and adding water to obtain 100 mL of solution.
8	A 3,500 ppm concentration solution was obtained by weighing 0.3500 g and adding water to obtain 100 mL of solution.
9	A 4,000 ppm concentration solution was obtained by weighing 0.4000 g and adding water to obtain 100 mL of solution.
10	A 4,500 ppm concentration solution was obtained by weighing 0.4500 g and adding water to obtain 100 mL of solution.

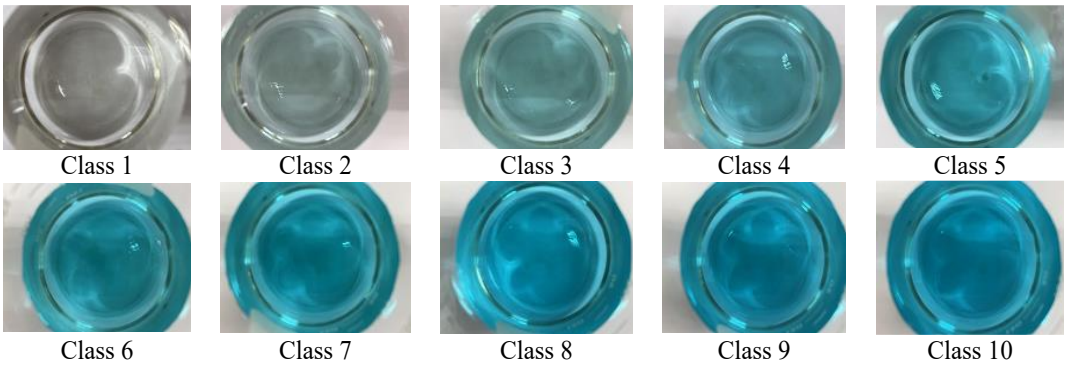

Figure 1 Examples of ten classes of the reference solutions

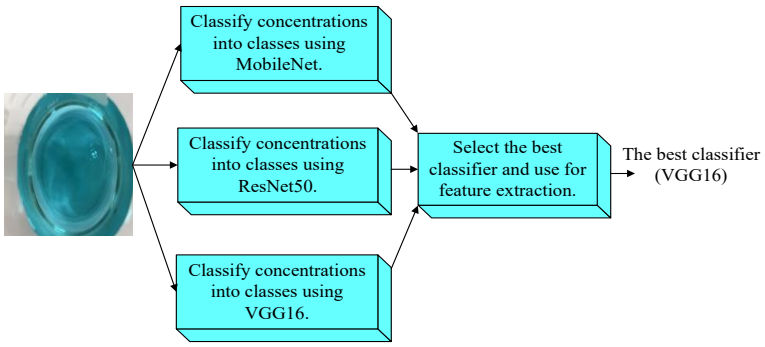

(a) Select the best deep learning concentration classifier.

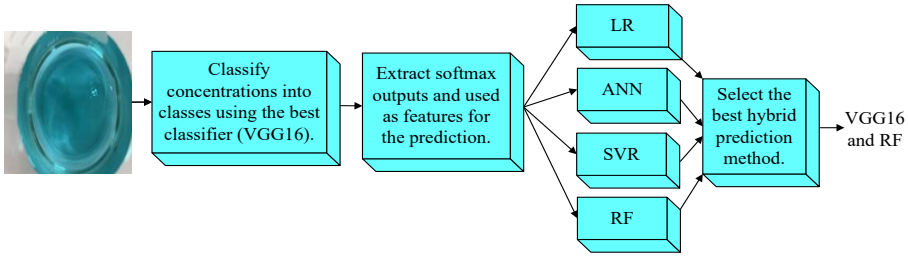

(b) Select the best machine learning concentration predictor.

Figure 2 A hybrid deep learning and machine learning framework for predicting aqueous solution concentrations.

In the first experimental phase, MobileNet, ResNet50, and VGG16 were each evaluated independently for classification performance. In the second phase, the softmax output features from the best-performing classifier (VGG16) were used as inputs to LR, ANN, SVR, and RF to identify the most accurate concentration predictor. The goal of the second part of the experiments was to determine the most effective machine learning model for predicting concentration levels based on features extracted using the best deep learning model.

4. Results

4.1 MobileNet, ResNet50, and VGG16 Model Accuracy and Loss

Figure 3 illustrates the accuracy and loss of MobileNet, ResNet50, and VGG16 after 300 epochs of training. The findings demonstrated that although MobileNet and ResNet50 had very good validation accuracy, it was not as high as that of VGG16. Compared with MobileNet, the loss of ResNet50 and VGG16 was more variable. Among MobileNet, ResNet50, and VGG16, VGG16 had the lowest validation loss after training.

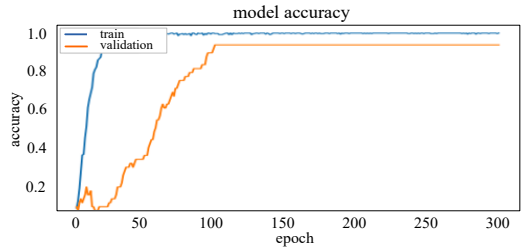

MobileNet model accuracy

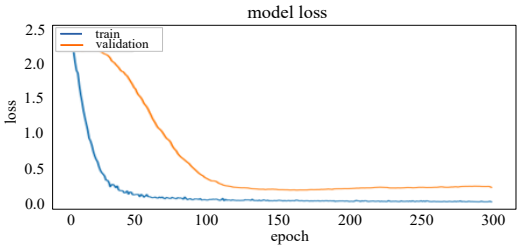

MobileNet model loss

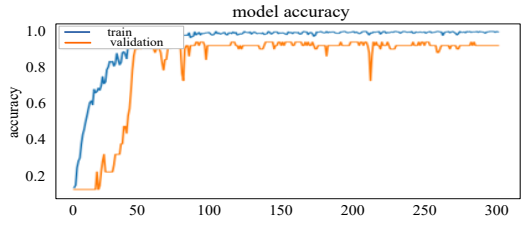

ResNet50 model accuracy

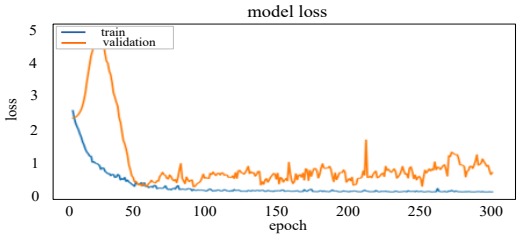

ResNet50 model loss

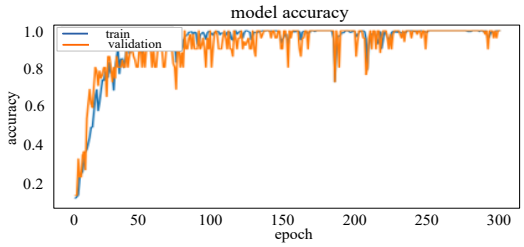

VGG16 model accuracy

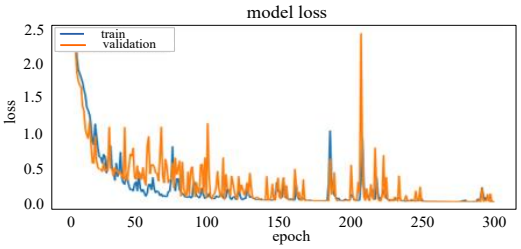

VGG16 model loss

Figure 3 Model accuracy and loss

Table 2 MobileNet confusion matrix when evaluating using the validation set

True \ Predicted	C1	C2	C3	C4	C5	C6	C7	C8	C9	C10
C1	40% (4)	60% (6)								
C2		100% (10)								
C3			100% (10)							
C4				100% (10)						
C5					100% (10)					
C6						100% (10)				
C7							100% (10)			
C8								100% (10)		
C9									100% (10)	
C10										100% (10)

4.2 MobileNet Classification Results

Table 2 presents the MobileNet confusion matrix derived from evaluation of the validation set. MobileNet accurately identified classes 2 through 9. However, 60% of class 1 images were categorized as class 2 images. Table 3 shows the MobileNet precision, recall, F1 score, macro average, and weighted average when evaluating using the validation set. The accuracy of 94% was achieved using MobileNet.

Table 4 presents the MobileNet confusion matrix derived from evaluation of the test set. Numerous inaccuracies occurred, particularly in the classification of class 1 images. All class 1 images were erroneously classified as class 2 images. 20% of class 6 images were erroneously classified as class 4 images, whereas 20% of class 6 images were mistakenly classified as class 8 images. For class 7 images, 60% were incorrectly classified as class 5 images. The results indicated that when MobileNet misclassified concentration classes, many classifications were assigned to classes that were not nearby, suggesting that reliably classifying concentration classes with MobileNet was quite difficult and utilizing the outputs from the final softmax layer of MobileNet as features for concentration prediction was inappropriate.

Table 5 presents MobileNet's classification performance on the test set. With an accuracy of only 80%, MobileNet was deemed unsuitable as a feature extractor for subsequent concentration prediction.

Table 3 MobileNet precision, recall, and F1 score when evaluating using the validation set

Class	precision	recall	F1 score	Class	precision	recall	F1 score
C1	1.0000	0.4000	0.5714	C6	1.0000	1.0000	1.0000
C2	0.6250	1.0000	0.7692	C7	1.0000	1.0000	1.0000
C3	1.0000	1.0000	1.0000	C8	1.0000	1.0000	1.0000
C4	1.0000	1.0000	1.0000	C9	1.0000	1.0000	1.0000
C5	1.0000	1.0000	1.0000	C10	1.0000	1.0000	1.0000
macro avg	0.9625	0.9400	0.9341				
weighted avg	0.9625	0.9400	0.9341				
accuracy		0.94					

Table 4 MobileNet confusion matrix when evaluating using the test set

True \ Predicted	C1	C2	C3	C4	C5	C6	C7	C8	C9	C10
C1		100% (10)								
C2		100% (10)								
C3			100% (10)							
C4				100% (10)						
C5					100% (10)					
C6				20% (2)		60% (6)		20% (2)		
C7					60% (6)		40% (4)			
C8								100% (10)		
C9									100% (10)	
C10										100% (10)

Table 5 MobileNet precision, recall, and F1 score when evaluating using the test set

Class	precision	recall	F1 score	Class	precision	recall	F1 score
C1	0.0000	0.0000	0.0000	C6	1.0000	0.6000	0.7500
C2	0.5000	1.0000	0.6667	C7	1.0000	0.4000	0.5714
C3	1.0000	1.0000	1.0000	C8	0.8333	1.0000	0.9091
C4	0.83333	1.0000	0.9091	C9	1.0000	1.0000	1.0000
C5	0.6250	1.0000	0.7692	C10	1.0000	1.0000	1.0000
macro avg	0.7792	0.8000	0.7576				
weighted avg	0.7792	0.8000	0.7576				
accuracy		0.8000					

Table 6 ResNet50 confusion matrix when evaluating using the validation set

True \ Predicted	C1	C2	C3	C4	C5	C6	C7	C8	C9	C10
C1	40% (4)	60% (6)								
C2		100% (10)								
C3			100% (10)							
C4				100% (10)						
C5					100% (10)					
C6						100% (10)				
C7							100% (10)			
C8								100% (10)		
C9									100% (10)	
C10										100% (10)

Table 7 ResNet50 precision, recall, and F1 score when evaluating using a validation set

Class	precision	recall	F1 score	Class	precision	recall	F1 score
C1	1.0000	0.4000	0.5714	C6	1.0000	1.0000	1.0000
C2	0.6250	1.0000	0.7692	C7	1.0000	1.0000	1.0000
C3	1.0000	1.0000	1.0000	C8	1.0000	1.0000	1.0000
C4	1.0000	1.0000	1.0000	C9	1.0000	1.0000	1.0000
C5	1.0000	1.0000	1.0000	C10	1.0000	1.0000	1.0000
macro avg	0.9625	0.9400	0.9341				
weighted avg	0.9625	0.9400	0.9341				
accuracy		0.94					

4.3 ResNet50 Classification Results

As shown in Table 6, ResNet 50 accurately identified classes 2 through 9. However, 60% of class 1 images were classified as class 2 images.

Table 7 shows the ResNet50 precision, recall, F1 score, macro average, and weighted average when evaluating the validation set. Compared with MobileNet, the same validation accuracy of 94% was achieved.

Table 8 presents the ResNet50 confusion matrix obtained from the evaluation of the test set. The accuracy was significantly lower than that obtained when evaluating the validation set. Numerous inaccuracies occurred, particularly in the classification of class 1 images. All class 1 images were erroneously classified as class 2 images. 80% of class 6 images were erroneously classified as other

classes. For class 7 images, 60% were incorrectly classified as class 8 images. The experimental results demonstrated that when ResNet50 misclassified concentration classes, numerous classifications were allocated to nonadjacent classes, indicating that accurately identifying concentration classes with ResNet50 was challenging. Using the outputs from the final softmax layer of ResNet50 as features for concentration prediction was unsuitable.

Table 9 presents the precision, recall, F1 score, macro average, and weighted average of ResNet50 as assessed using the test set. The test set yielded an accuracy of 78%. The results indicated that ResNet50 attained an accuracy of 78% on the test set, which was insufficient for subsequent use in predicting solution concentrations.

Table 8 ResNet50 confusion matrix when evaluating the test set

True \ Predicted	C1	C2	C3	C4	C5	C6	C7	C8	C9	C10
C1		100% (10)								
C2		100% (10)								
C3			100% (10)							
C4				100% (10)						
C5					100% (10)					
C6				20% (2)		40% (4)		20% (2)	40% (4)	
C7							40% (4)	60% (6)	0%	
C8								100% (10)	0%	
C9									100% (10)	
C10										100% (10)

Table 9 ResNet50 precision, recall, and F1 score when evaluating using a test set

Class	precision	recall	F1 score	Class	precision	recall	F1 score
C1	0.0000	0.0000	0.0000	C6	1.0000	0.4000	0.5714
C2	0.5000	1.0000	0.6667	C7	1.0000	0.4000	0.5714
C3	1.0000	1.0000	1.0000	C8	0.5556	1.0000	0.7143
C4	1.0000	1.0000	1.0000	C9	0.7143	1.0000	0.8333
C5	1.0000	1.0000	1.0000	C10	1.0000	1.0000	1.0000
macro avg	0.7770	0.7800	0.7357				
weighted avg	0.7770	0.7800	0.7357				
accuracy	0.7800						

4.4 VGG16 Classification Results

Table 10 presents the VGG16 confusion matrix derived from evaluation of the validation set. The validation results indicated that VGG16 could accurately classify images of all classes.

VGG16 outperformed MobileNet and ResNet50 in classification. An accuracy of 100% was attained on the validation set. Precision, recall, F1 score, macro average, and weighted average values of 1.0000 were achieved across all classes. Table 11 presents the VGG16 confusion matrix derived from the evaluation of the test set. Only a few classification errors were found in class 6 images. 20% of class 6 images were erroneously classified as class 7 images. For evaluating using the test set, VGG16 performed better than MobileNet and ResNet50.

Table 10 VGG16 confusion matrix when evaluating using a validation set

True \ Predicted	C1	C2	C3	C4	C5	C6	C7	C8	C9	C10
C1	100% (10)									
C2		100% (10)								
C3			100% (10)							
C4				100% (10)						
C5					100% (10)					
C6						100% (10)				
C7							100% (10)			
C8								100% (10)		
C9									100% (10)	
C10										100% (10)

Table 11 VGG16 confusion matrix when evaluating using a test set

True \ Predicted	C1	C2	C3	C4	C5	C6	C7	C8	C9	C10
C1	100% (10)									
C2		100% (10)								
C3			100% (10)							
C4				100% (10)						
C5					100% (10)					
C6						80% (8)	20% (2)			
C7							100% (10)			
C8								100% (10)		
C9									100% (10)	
C10										100% (10)

Table 12 displays the precision, recall, F1 score, macro average, and weighted average of VGG16 as assessed using the test set. The accuracy was 98%, with macro average and weighted average values for precision, recall, and F1 score of 0.9833, 0.9800, and 0.9798, respectively.

Compared with MobileNet and ResNet50, VGG16 was more efficient in classifying images of solutions with 10 different concentration levels. Therefore, in the next part, ten features derived from the VGG16 softmax layer were used with LR, ANN, SVR, and RF to predict the concentrations.

4.5 Concentration Prediction Using Machine Learning Predictors

Figures 4–9 illustrate the true and predicted values when using the VGG16 softmax features with LR, ANN, SVR with different kernel functions, and RF for prediction. The results revealed that RF outperformed LR, ANN, SVR with a linear kernel function, SVR with a polynomial kernel function, and SVR with a radial basis kernel function.

Table 12 VGG16 precision, recall, and F1 score when evaluating using a test set

Class	precision	recall	F1 score	Class	precision	recall	F1 score
C1	1.0000	1.0000	1.0000	C6	1.0000	0.8000	0.8889
C2	1.0000	1.0000	1.0000	C7	0.8333	1.0000	0.9091
C3	1.0000	1.0000	1.0000	C8	1.0000	1.0000	1.0000
C4	1.0000	1.0000	1.0000	C9	1.0000	1.0000	1.0000
C5	1.0000	1.0000	1.0000	C10	1.0000	1.0000	1.0000
macro avg	0.9833	0.9800	0.9798				
weighted avg	0.9833	0.9800	0.9798				
accuracy		0.9800					

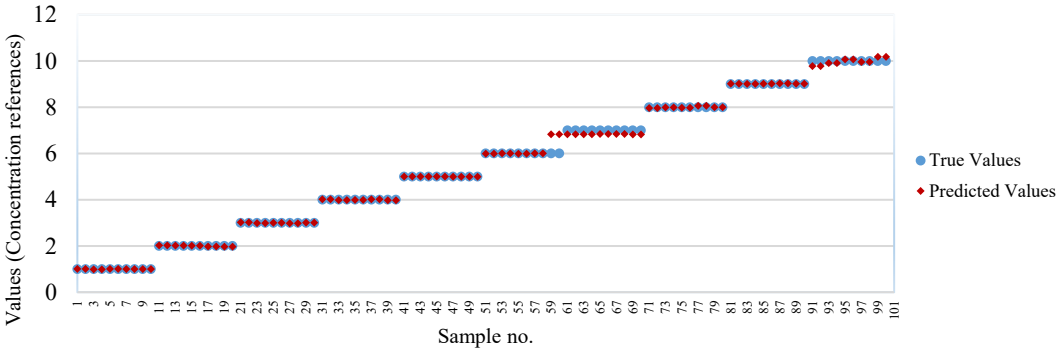

Figure 4 True and predicted values when using VGG16 softmax values and LR to evaluate the test set

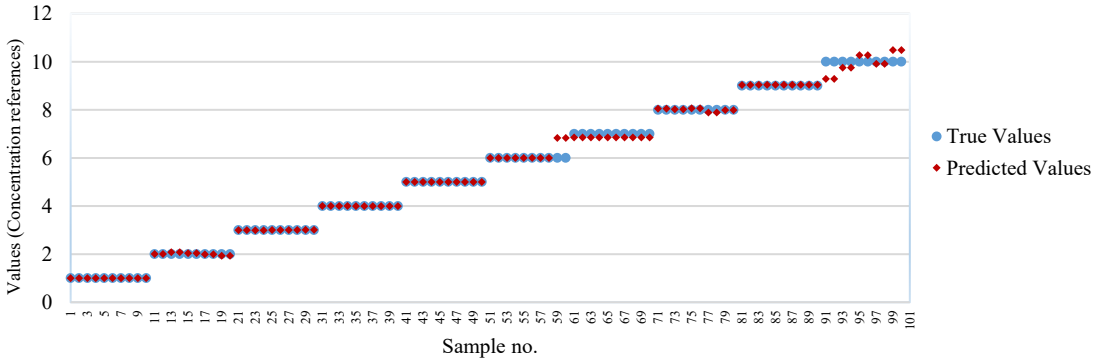

Figure 5 True and predicted values when using VGG16 softmax values and ANN to evaluate the test set

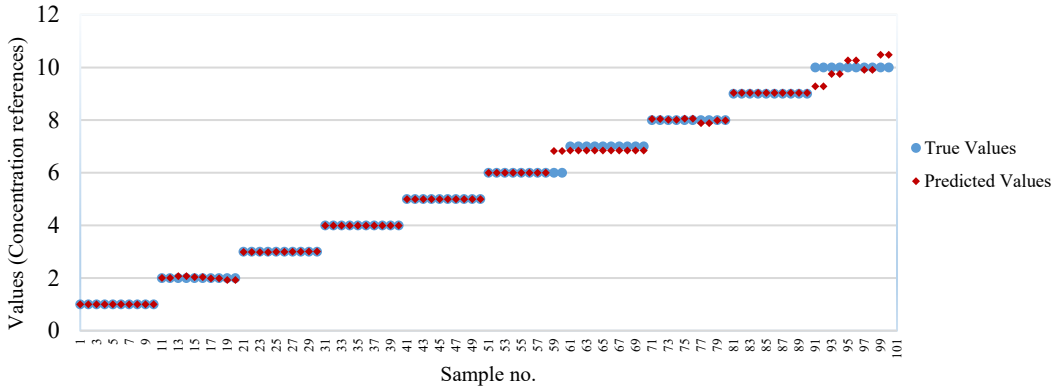

Figure 6 True and predicted values when using VGG16 softmax values and SVR with a linear kernel to evaluate the test set

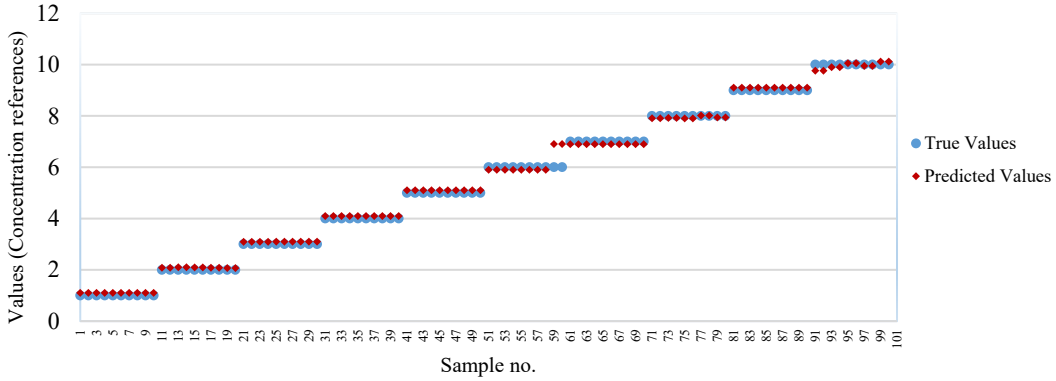

Figure 7 True and predicted values when using VGG16 softmax values and SVR with a polynomial kernel to evaluate the test set

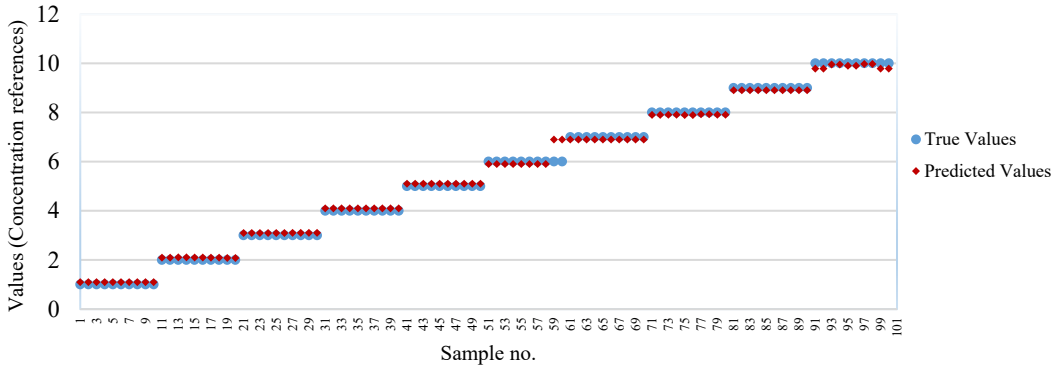

Figure 8 True and predicted values when using VGG16 softmax values and SVR with a radial basis kernel to evaluate the test set

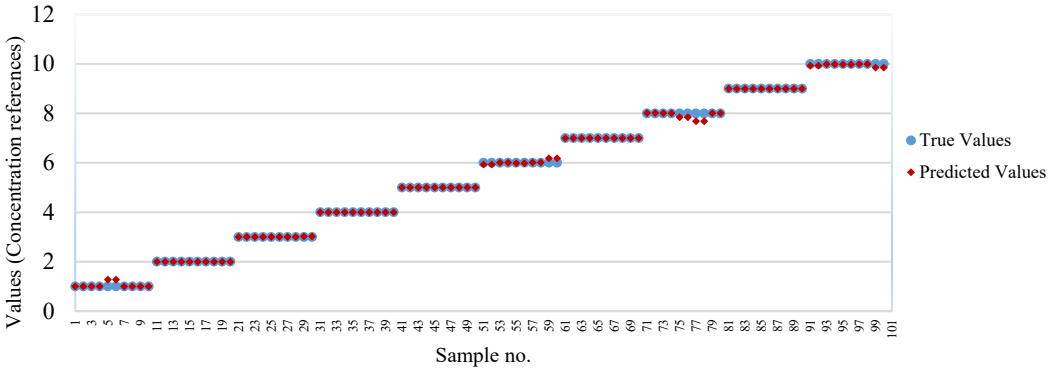

Figure 9 True and predicted values when using VGG16 softmax values and RF to evaluate the test set.

Table 13 shows the absolute errors, relative errors, percentage errors, and Root Mean Squared Error (RMSE) in concentration prediction. The findings demonstrated that RF was the most accurate predictor, with absolute errors, relative errors, percentage errors, and RMSE of 0.026640, 0.008322, 0.832174, and 0.072531, respectively.

4.6 Concentration Prediction Performance on Absolute (ppm) Scale

The concentrations from class 1 to class 10 were uniformly varied from 0 ppm to 4500 ppm. Utilizing VGG16 for feature extraction and RF for concentration prediction yielded an average absolute error of 13.32 ppm and RMSE of 36.3056 ppm. A high R^2 value of 0.999361 was attained, although prediction errors were observed at specific concentration levels, particularly 0 ppm and 3500 ppm. Figure 10 illustrates the true and predicted values derived from VGG16 softmax outputs and RF predictions. The findings demonstrated that the proposed technique was effective in forecasting solution concentrations.

The paired sample statistical t-test revealed no significant difference between the true and predicted concentration levels.

Table 13 Errors in the concentration prediction

Predictor	Absolute errors	Relative errors	Percentage errors	RMSE
LR	0.056229	0.009593	0.959259	0.137079
ANN	0.080000	0.010000	1.190000	0.185881
Linear kernel SVR	0.112172	0.030762	3.076165	0.161342
Polynomial kernel SVR	0.220849	0.042730	4.272986	0.456836
Radial basis kernel SVR	0.116940	0.031844	3.184445	0.164166
RF	0.026640	0.008322	0.832174	0.072531

Table 14 The paired sample statistical t-test result calculated from the true and predicted concentration values

		Paired Differences					*t*	df	Sig. (2-tailed)
		Mean	Std. Deviation	Std. Error Mean	95% Confidence Interval of the Difference				
					Lower	Upper			
Pair 1	True Values - Predicted Values	2.9600	36.3671	3.6367	-4.2560	10.1760	.814	99	.418

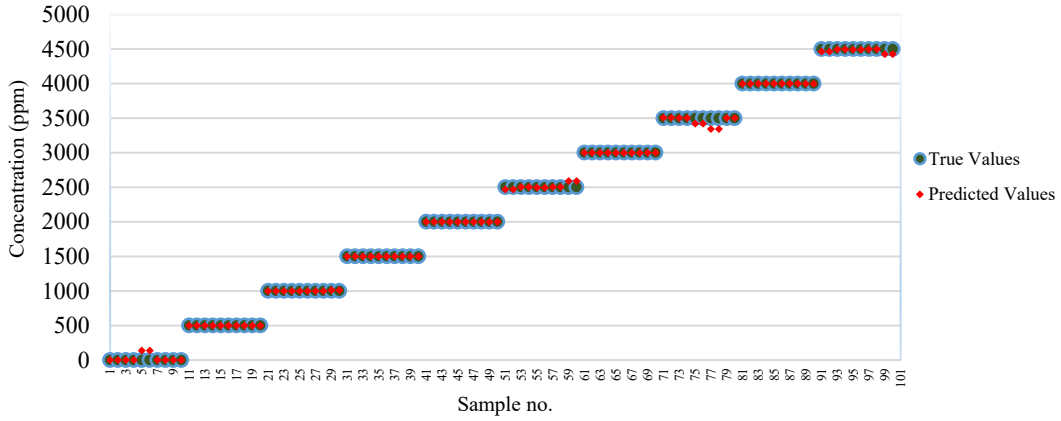

Figure 10 True and predicted values when using VGG16 softmax values and RF to predict concentration values.

5. Discussion

This work suggested a hybrid deep learning and machine learning approach for predicting aqueous solution concentrations. VGG16 was chosen for concentration classification and feature extraction. Despite the extensive training period for VGG16, the time required for classification or feature extraction was not very high. Although RF is less commonly used in some classification tasks than ANN and SVM for classification problems, empirical evidence from this and prior studies suggests that RF is a highly effective ensemble learning approach for regression and predictive tasks. Therefore, we integrated RF into our experiments. RF required minimal time for both training and prediction. The results corroborated the finding of Dong and Phoophuangpairoj (2024) that VGG16 is an effective deep learning model for image classification tasks. While MobileNet effectively classified banana ripeness from photos (Chen & Phoophuangpairoj, 2024), it failed to reliably classify solution concentrations. ANN and RF were effective for classifying hazardous motorcycling (Si & Phoophuangpairoj, 2025). Linear SVM was identified as a high-performing classifier for lung cancer prediction (Pechprasarn et al., 2024) and diabetes classification (Pechprasarn et al., 2025), while SVR was applied to temperature forecasting under distinct climate scenarios (Miftahurrohmah et al., 2025). However, in this study, SVR with various kernel functions failed to achieve lower prediction errors than RF, LR, or ANN. We concur with Tun et al. (2021) that the application of hybrid approaches, such as VGG16, CNN, and SVM, was noteworthy regarding accuracy. A fixed number of features is used to train ANN and SVM. In contrast, RF uses random subsets of features to build multiple trees during training. Then, it aggregates the output of these trees using a voting mechanism, leveraging the knowledge from multiple trees to ensure accurate results. In light of this, we also recommend combining deep learning techniques with RF as an efficient approach. Using deep learning and machine learning in chemistry is appealing due to cost-effectiveness and efficiency, especially for applications that do not require highly precise measurements from expensive equipment. Despite the minimal prediction errors, we validated the efficacy of our method using a paired t-test. The paired t-test yielded $p = .418$ (two-tailed), indicating that the null hypothesis could not be rejected at the conventional significance threshold of $\alpha = 0.05$. This result indicated insufficient evidence to determine that a statistically significant difference exists between the means of the two paired samples (true concentration values and predicted values). Consequently, the proposed method was applicable for determining the concentration levels of the aqueous solutions.

Traditional techniques for determining concentrations, such as spectrophotometry or chemical titration, usually require costly chemicals and sophisticated equipment. In contrast, estimating solution concentration using photographic analysis offers a more accessible and affordable option. Image-based approaches are particularly appealing for routine analysis or field applications where resources are limited due to their lower cost and ease of use. In addition, compared with image processing techniques, including threshold extraction and analysis of RGB values to obtain multicolor feature indices (Dai et al., 2025), the proposed inexpensive method has the

advantage of learning from data and being simpler to implement when solutions have different colors, which may improve generalizability when applied to other solutions. Using 600 image samples to forecast concentrations across ten unique categories may be inadequate. In the future, more images should be incorporated and analyzed. The proposed method can also be employed to identify residues, such as pesticides, using test strips for rapid detection. The color of the solution may affect the effectiveness of the proposed method. Additional research on solutions with various colors is necessary for broader real-world applications, such as environmental monitoring and food safety kits.

6. Conclusion

This study examined image-based methods for predicting aqueous solution concentrations. MobileNet, ResNet50, and VGG16 were studied for classifying the concentration classes. LR, ANN, SVR, and RF were studied for predicting concentration levels using features extracted from the final softmax layer of VGG16. The first part of the experiments revealed that VGG16 outperformed MobileNet and ResNet50 in classifying images into ten concentration classes. MobileNet achieved higher accuracy than ResNet50 when evaluated using the test set. Based on the absolute, relative, and percentage errors, the results indicated that RF was the most accurate predictor. The second-best predictor was LR. ANN and SVR with a linear kernel function came next. In addition to achieving low errors, the t-test was employed to validate the efficacy of the proposed method. According to the experiment's findings, we proposed a hybrid strategy that combined a deep learning feature extractor using VGG16 with a machine learning predictor using RF. The efficacy of the approach warrants further examination with alternative chemicals. This approach is cost-effective; however, a constraint is that the solution's color must vary with its concentration.

7. Abbreviations

Abbreviation	Full Term
AAS	Atomic Absorption Spectroscopy
ANN	Artificial Neural Network
CNN	Convolutional Neural Network
Cu^{2+}	Copper Ion
HPLC	High-Performance Liquid Chromatography
HSV	Hue, Saturation, Value
ICP-MS	Inductively Coupled Plasma Mass Spectrometry
LR	Linear Regression
L2	L2 Regularization
lx	Lux (the unit of illuminance)
ReLU	Rectified Linear Unit
RF	Random Forest
RGB	Red, Green, Blue
RMSE	Root Mean Squared Error
R^2	Coefficient of Determination
SVM	Support Vector Machine
SVR	Support Vector Regression
VGG16	Visual Geometry Group 16-layer Convolutional Neural Network
YOLO	You Only Look Once

8. CRediT Statement

Rong Phoophuangpairoj: Conceptualization, Methodology, Software, Validation, Formal Analysis, Investigation, Resources, Writing – Original Draft, Writing – Review & Editing, Visualization, Project Administration.
Panida Charnkeitkong: Conceptualization, Validation, Investigation, Resources, Data Curation, Writing – Original Draft, Writing – Review & Editing, Visualization.

9. References

Chen, H., & Phoophuangpairoj, R. (2024). Determining Banana Ripeness Using MobileNet [Conference presentation]. *2024 12th International Electrical Engineering Congress (iEECON)*. IEEE, Pattaya, Thailand. https://doi.org/10.1109/iEECON60677.2024.10537906

Dai, J., Chen, X., Zhang, Y., Zhang, M., Dong, Y., Zheng, Q., ... & Zhao, Y. (2025). Machine learning-enhanced color recognition of test strips for rapid pesticide residue detection in fruits and vegetables. *Food Control*, *174*, Article 111256. https://doi.org/10.1016/j.foodcont.2025.111256

Dong, X., & Phoophuangpairoj, R. (2024). Mango Maturity Classification using VGG16 [Conference presentation]. *2024 12th International Electrical Engineering Congress*

(iEECON). IEEE, Pattaya, Thailand. https://doi.org/10.1109/iEECON60677.2024.10537862

Feng, K., Zhai, M. Y., Wei, Y. S., Zong, M. H., Wu, H., & Han, S. Y. (2021). Fabrication of nano/micro-structured electrospun detection card for the detection of pesticide residues. *Foods*, *10*(4), Article 889. https://doi.org/10.3390/foods10040889

Guo, K., Shen, Y., Gonzalez-Montiel, G. A., Huang, Y., Zhou, Y., Surve, M., ... & Zhang, X. (2025). Artificial intelligence in spectroscopy: Advancing chemistry from prediction to generation and beyond. *arXiv preprint arXiv:2502.09897*. https://doi.org/10.48550/arXiv.2502.09897

Han, Q., Yang, X., Huo, Y., Lu, J., & Liu, Y. (2023). Determination of ultra-trace amounts of copper in environmental water samples by dispersive liquid-liquid microextraction combined with graphite furnace atomic absorption spectrometry. *Separations*, *10*(2), Article 93. https://doi.org/10.3390/separations10020093

Han, Y., Tian, Y., Li, Q., Yao, T., Yao, J., Zhang, Z., & Wu, L. (2025). Advances in detection technologies for pesticide residues and heavy metals in rice: A comprehensive review of spectroscopy, chromatography, and biosensors. *Foods*, *14*(6), Article 1070. https://doi.org/10.3390/foods14061070

Li, Z., Liu, H., Wang, C., Chen, J., & Zhang, Q. (2022). Research on performance optimization of liquid concentration detection systems based on turbulence elimination. *Processes*, *11*(1), Article 85. https://doi.org/10.3390/pr11010085

Miftahurrohmah, B., Cholilie, I. A., Wijaya, S. U., Atmaja, F., Bariyah, T., & Wulandari, C. (2025). Future growing seasons: Bias correction with SVR and QDM for Indonesian temperature projection under RCP 2.6 and RCP 8.5. *Journal of Current Science and Technology*, *15*(2), Article 100. https://doi.org/10.59796/jcst.V15N2.2025.100

Paredes, C., Ahumada, D., & Ágreda, J. (2023). Gravimetric complexometric titration method to determine mass fraction of ethylenediaminetetraacetic acid disodium salt dihydrate in candidate-certified reference materials. *MAPAN-Journal of Metrology Society of India*, *38*(1), 179-191. https://doi.org/10.1007/s12647-022-00602-0

Pechprasarn, S., Srisaranon, N., & Yimluean, P. (2025). Optimizing diabetes prediction: An evaluation of machine learning models through strategic feature selection. *Journal of Current Science and Technology*, *15*(1), Article 75. https://doi.org/10.59796/jcst.V15N1.2025.75

Pechprasarn, S., Suechoey, N., Pholtrakoolwong, N., Tanedvorapinyo, P., & Toboonliang, Y. (2024). Optimizing lung cancer diagnosis with machine learning and feature selection methods. *Journal of Current Science and Technology*, *14*(3), Article 55. https://doi.org/10.59796/jcst.V14N3.2024.55

Qi, M., & Phoophuangpairoj, R. (2024). Classification of snatch weightlifting phases [Conference presentation]. *2024 12th International Electrical Engineering Congress (iEECON)*. IEEE, Pattaya, Thailand. https://doi.org/10.1109/iEECON60677.2024.10537843

Sharma, C., Sharma, K., Trivedi, P., Sharma, S., & Yadav, N. (2025). Solvent extraction and trace analysis of as (III) in alloys, biological, and environmental samples by spectrophotometry and ICP-MS. *Discover Chemistry*, *2*(1), Article 30. https://doi.org/10.1007/s44371-025-00108-z

Si, R., & Phoophuangpairoj, R. (2025). Detection of dangerous motorcycling using YOLO and machine learning classifiers. *ECTI Transactions on Computer and Information Technology*, *19*(2), 294-306. https://doi.org/10.37936/ecti-cit.2025192.259018

Sun, D., Ma, X., Chang, J., Zhang, G., Su, M., Sikorski, M., ... & Bai, X. (2024). Analysis of trace heavy metal in solution using liquid cathode glow discharge spectroscopy. *Sensors*, *24*(23), Article 7756. https://doi.org/10.3390/s24237756

Tun, N. L., Gavrilov, A., Tun, N. M., Trieu, D. M., & Aung, H. (2021). Remote sensing data classification using a hybrid pre-trained VGG16 CNN-SVM classifier [Conference presentation]. *2021 IEEE Conference of Russian Young Researchers in Electrical and Electronic Engineering (ElConRus).* IEEE, St. Petersburg, Moscow, Russia. https://doi.org/10.1109/ElConRus51938.2021.9396706

Xhanari, K., & Finšgar, M. (2023). Recent advances in the modification of electrodes for trace metal analysis: A review. *Analyst*, *148*(23), 5805-5821. https://doi.org/10.1039/D3AN01252B

Zhang, Y., Zheng, Q., Chen, X., Guan, Y., Dai, J., Zhang, M., ... & Tang, H. (2023). Comparison and analysis of several quantitative identification models of pesticide residues based on quick detection paperboard. *Processes*, *11*(6), Article 1854. https://doi.org/10.3390/pr11061854

Zhong, J., Wang, Z., Chen, Y., Huan, W., Shi, M., Lei, L., ... & Chen, L. (2024). Determination of trace heavy metal elements in litterfall by inductively coupled plasma optical emission spectrometry after extraction using choline chloride-based deep eutectic solvents. *RSC Advances*, *14*(31), 22497-22503. https://doi.org/10.1039/D4RA02573C